

A facile one-pot synthesis of polyaniline/magnetite nanocomposites by micelles-assisted method

K. Basavaiah · Y. Pavan Kumar · A. V. Prasada Rao

Received: 30 April 2012 / Accepted: 16 July 2012 / Published online: 7 August 2012
© The Author(s) 2012. This article is published with open access at Springerlink.com

Abstract Magnetic nanocomposites based on polyaniline (PANI) and magnetite nanoparticles (Fe_3O_4 NPs) have been prepared by an in situ self-assembly method in presence of dodecylbenzene sulfonic acid (DBSA) as dopant as well as surfactant. Influence of the aniline to DBSA molar ratio on morphology, magnetic properties, and thermal stability of PANI/ Fe_3O_4 NPs composites has been investigated. Spectroscopic results indicated the interaction between PANI nanorods and Fe_3O_4 NPs. Scanning electron microscopy and transmission electron microscopy images indicated that PANI rods were decorated with Fe_3O_4 NPs. Morphologies of nanocomposites were found to be critically dependent on molar ratios of organic acid to monomer. PANI nanorod/ Fe_3O_4 NPs composites showed superparamagnetism and higher thermal stability with small mass fraction of Fe_3O_4 NPs.

Keywords Intrinsic conducting polymer · Polyaniline · Magnetite nanoparticle · Superparamagnetism

Introduction

Since their discovery, intrinsic conducting polymers (ICPs) have received great attention because of their unique properties coupled with potential technological applications. Compared to other ICPs, polyaniline (PANI) has been the most extensively studied system due to its electrical and electrochemical properties, good environmental stability, high conductivity in doped form, low monomer cost, ease of

polymerization and useful for potential applications in energy storage devices, electron field emitters, chemical and biological sensors, actuators, etc. (Wu and Bein 1994; Wang et al. 2001; Zhang et al. 2004; Hatchett and Josowicz 2008; Li et al. 2009). More recently multifunctional nanocomposites based on PANI nanostructures, such as nanotubes, nanofibers, nanowires, and nanorods combined with magnetic nanoparticles have also been investigated for applications such as EMI shielding, catalysis, anti-biofouling, immunity assay, separation and purification of biomolecules, carriers for targeted drug delivery, biosensors and electromagnetic device applications have been reported (Ugelstad et al. 1992; McMichael et al. 1992; Marchessault et al. 1992; Bhatnagar and Rosensweig 1995). Among the various magnetic dispersions, magnetite nanoparticles (Fe_3O_4 NPs) are useful because of their low toxicity, high saturation magnetization (Raj et al. 1995; Batlle and Labarta 2002; Wilson et al. 2004). All these applications require the Fe_3O_4 NPs to be chemically stable with uniform particle size, and well dispersed in aqueous medium. Nevertheless, preparation of stable Fe_3O_4 NPs is a challenge as the nanoparticles possess high surface area to volume ratios and tend to aggregate to reduce their surface energy. In addition, the strong magnetic dipole–dipole interaction and Vander Waal’s attractive forces among the nanoparticles also cause the particles to aggregate (Gupta and Gupta 2005). Consequently, these materials show poor magnetic properties and low dispersibility. One of the important strategies to overcome the above limitations is to shield the Fe_3O_4 NPs by coating them with macrocyclic surfactants, polymers, inorganic metals, or oxides (Jeong et al. 2007). The surrounding layer around each particle not only avoids further aggregation but also provides a useful platform for more functionalization.

Various synthetic methods have been reported for obtaining magnetic Fe_3O_4 /PANI composites, which include

K. Basavaiah (✉) · Y. Pavan Kumar · A. V. Prasada Rao
Department of Inorganic and Analytical Chemistry,
Andhra University, Visakhapatnam 530003, India
e-mail: klbasu@gmail.com

direct precipitation of iron salt in a solution of polymer, oxidative chemical polymerization, the in situ synthesis of polymer via an oxidative or electrochemical procedure in presence of well-dispersed magnetic nanoparticles (Bai and Shi 2007; Zhang and Wan 2003). Fabrication of thin films of PANI/ γ - Fe_2O_3 using anionic surfactants has also been reported (Mallikarjuna et al. 2005). Raksha et al. (2005) reported Fe_3O_4 /PANI nanocomposites prepared by mixing aqueous solutions of iron (II) sulfate and 1-methyl-2-pyrrolidinone (NMP) solutions of PANI at different pH values. The precipitate obtained from acidic conditions (e.g., at pH = 1) was found to contain a low concentration of Fe_3O_4 (Wan and Li 1997). Fe_3O_4 /PANI nanocomposites were also prepared by other means such as modification-redoping method, high-energy ball milling method, precipitation–oxidation technique, and chemical oxidative copolymerization of aniline and 5-amino-2-naphthalenesulfonic acid in presence of Fe_3O_4 NPs (Deng et al. 2002; Yang et al. 2003; Bao and Jiang 2005; Reddy et al. 2007). The obtained nanocomposites showed ferromagnetic behavior with saturation magnetization 9.7 emu g^{-1} . Nanocomposite particles that are prepared by these methods typically showed a significant particle size distribution, containing non-uniform magnetite fraction in composite with aggregates of iron oxide leading to an uncontrolled structure and irreproducible material properties.

In this paper, we report the synthesis of magnetic and conducting polymer composites based on Fe_3O_4 NPs on DBSA-doped PANI matrix using ammonium persulfate (APS) as an oxidant in presence of dodecylbenzenesulfonic acid (DBSA) via self-assembly method. The influence of DBSA content on the morphology and magnetic properties of resulting nanocomposites are also investigated.

Experimental details

Materials and methods

Aniline and DBSA were purchased from Aldrich. Aniline was double distilled under reduced pressure and stored at $0\text{--}5^\circ\text{C}$. Other reagents viz ammonium persulfate [APS , $(\text{NH}_4)_2\text{S}_2\text{O}_8$], ferric chloride hexahydrate ($\text{FeCl}_3\cdot 6\text{H}_2\text{O}$), iron (II) sulfate heptahydrate ($\text{FeSO}_4\cdot 7\text{H}_2\text{O}$), ammonia ($\text{NH}_3 \text{ H}_2\text{O}$), sodium hydroxide and methanol were of AR grade from Merck, India and all these chemicals were used as received without any further purification. Milli-Q water with resistance greater than $18 \text{ M}\Omega$ was used for the preparation of all solutions.

Surface morphology was examined by scanning electron microscopy (SEM) using JEOL-JSM6610 LV equipped with an electron probe-micro analyzer. Transmission electron microscopy images were obtained (TEM model FEI TECNAI G2 S-Twin) at an accelerating voltages of 120 and 200 kV. X-ray diffraction patterns (XRD) were

collected using a Siemens AXS D5005 X-ray diffractometer at 1 degree per minute with Cu-K α radiation. Fourier transform infrared (FTIR) spectra were recorded over the range of $400\text{--}4,000 \text{ cm}^{-1}$ using a Perkin Elmer SPECTRUM 1000 FTIR Spectrometer. Powder samples were mixed thoroughly with KBr and pressed into thin pellets. For UV–Visible absorption spectra, the samples were dissolved in dimethylsulfoxide (DMSO) and spectra were recorded on a Perkin-Elmer double beam LS-50 spectrophotometer. Room temperature magnetization measurements versus applied magnetic field were carried out using VSM, Lakeshore 665, USA. Thermogravimetric analysis (TGA) was done using, Cahn TG131 system with a heating rate of $20^\circ\text{C min}^{-1}$ under N_2 atmosphere.

Preparation of DBSA-doped PANI/ Fe_3O_4 nanocomposites

The DBSA-doped PANI/ Fe_3O_4 nanocomposite was synthesized as follows. In a typical experiment, 0.093 g of aniline was added drop wise to 1 ml of DBSA contained in 50 ml of Milli Q water under vigorous stirring. The reaction mixture was quickly cooled to $0\text{--}5^\circ\text{C}$ using ice-water bath with constant stirring for 2 h to obtain a milky dispersion of particles of anilinium–DBSA complex. Then, a pre-cooled solution of 1 ml aqueous ammonium persulfate (1 mol/L) was added dropwise to the above under vigorous stirring. The color of the reaction mixture slowly turns from colorless to light blue and eventually to dark green. After the addition is complete, reaction mixture is maintained at $0\text{--}5^\circ\text{C}$ for 5 h, before allowing it to attain room temperature to yield DBSA-doped PANI. Then, 10 ml of 1 mol L^{-1} $\text{FeCl}_3\cdot 6\text{H}_2\text{O}$ and 10 ml of 0.5 mol L^{-1} $\text{FeSO}_4\cdot 7\text{H}_2\text{O}$ aqueous solutions were rapidly injected into the above reaction mixture and slowly heated up to 65°C under stirring, followed by the addition of 5 ml of 25 % NH_4OH . Color of the reaction mixture turns black indicating the formation of magnetite. The reaction mixture was suggested to vigorous stirring for 5 h until a very viscous PANI/ Fe_3O_4 NPs nanocomposite was obtained. The obtained product was centrifuged washed with distilled water followed by methanol and dried under vacuum at room temperature for 12 h. The same procedure has been adopted for preparation of all DBSA-doped PANI/ Fe_3O_4 NPs composites, except for varying the molar ratio of DBSA to aniline from 1:1 to 1:5.

Results and discussions

Synthesis of PANI nanorods/ Fe_3O_4 NPs composite is based on the oxidative chemical polymerization of aniline in an

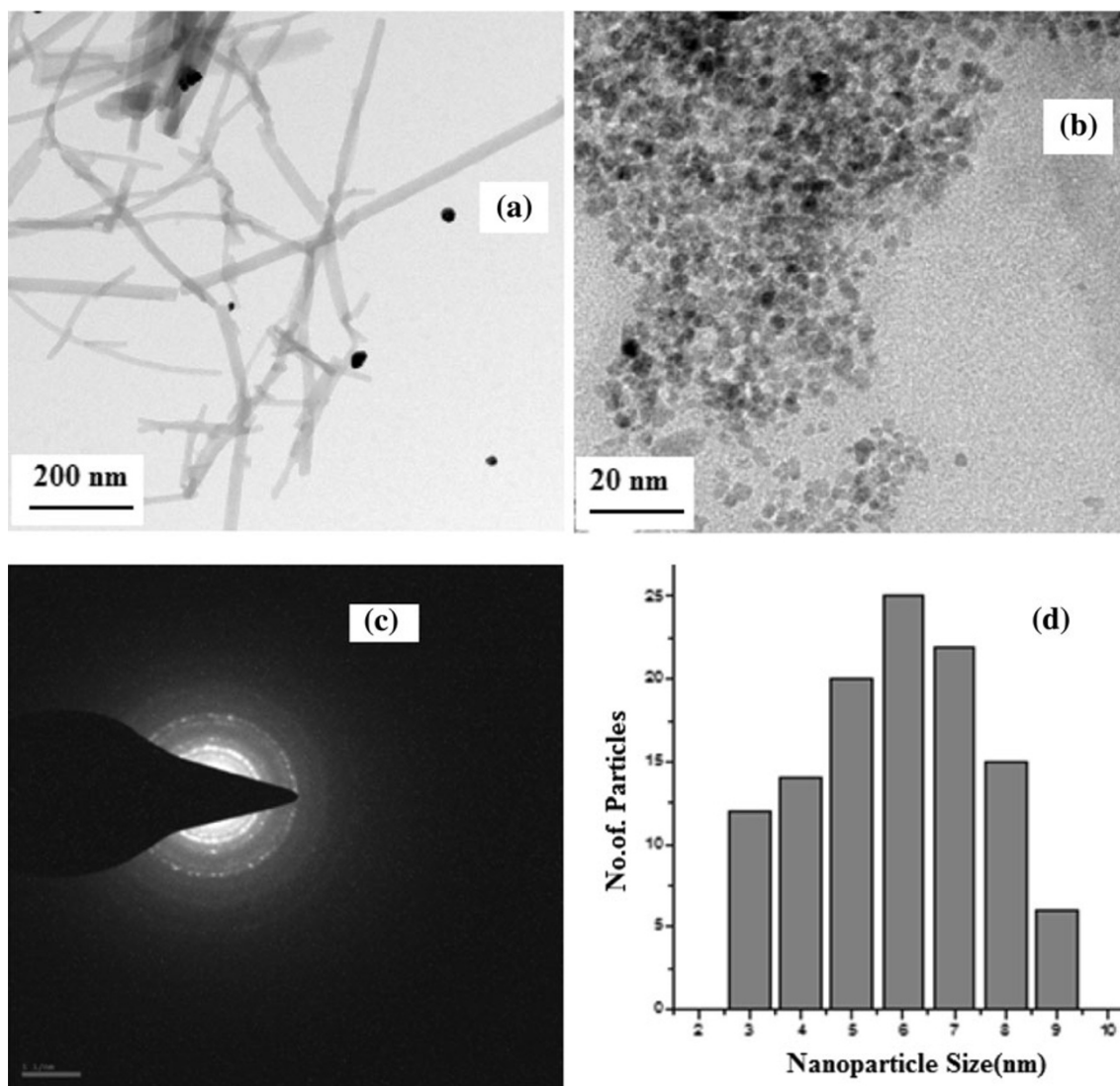


Fig. 1 TEM micrographs of PANI/Fe₃O₄-composites **a** crude reaction dispersion, **b** powder redispersed in dimethylsulfoxide, **c** selected area electron diffraction pattern, and **d** particle size distribution histogram

acidic environment using ammoniumpersulfate (APS) as the oxidant in presence of a surfactant. In the present study, DBSA is used as a surfactant. In aqueous solution, DBSA forms micelles due to its hydrophilic group ($-\text{SO}_3\text{H}$) and hydrophobic alkyl group. DBSA also forms dopant-aniline salts with aniline, which act as “soft template” for growth of PANI rods. With progressive polymerization growth of nanorods is controlled by elongation process and of excess DBSA present prevents the formation of larger particles via steric hindrance and limit PANI rods to nanometer size. Fe₃O₄ NPs formed inside DBSA micelle reactor during sedimentation process get inserted on to the PANI rods. $-\text{SO}_3^-$ groups of DBSA limits the size of Fe₃O₄ NPs by forming of a protection layer around the particle through the hydrophilic $-\text{SO}_3^-$ group. Aggregation of such particles is arrested by the repulsive forces due to the hydrophilic alkyl groups surroundings each particle.

TEM micrographs of as prepared crude PANI/Fe₃O₄ and final dried powder after in dispersed in dimethyl sulfoxide (DMSO), are presented in Fig. 1. TEM micrographs depicted in Fig. 1 clearly show the rod like morphology of PANI with average diameter ranging from 18 to 45 nm and length a few hundred nanometres. TEM image of composite samples (Fig. 1b) shows that the Fe₃O₄ NPs are of 5–8 nm in size. Electron diffraction (ED) pattern obtained from the particles given in Fig 1c is in good agreement with the characteristic electron diffraction pattern of Fe₃O₄ NPs of spinel structure. Figure 1d shows the particle size distribution of Fe₃O₄ NPs in the composite.

Morphology evolution of DBSA-doped PANI/Fe₃O₄ NPs composites for different molar ratios of DBSA to aniline is shown in Fig. 2. From the SEM images (Fig. 2a, b) it can be seen that the rod-like morphology of PANI is obtained for 1:5 molar ratio of DBSA to aniline. Composite samples prepared with 1:4, 1:3, and 1:1 molar ratios of DBSA to aniline, shown in

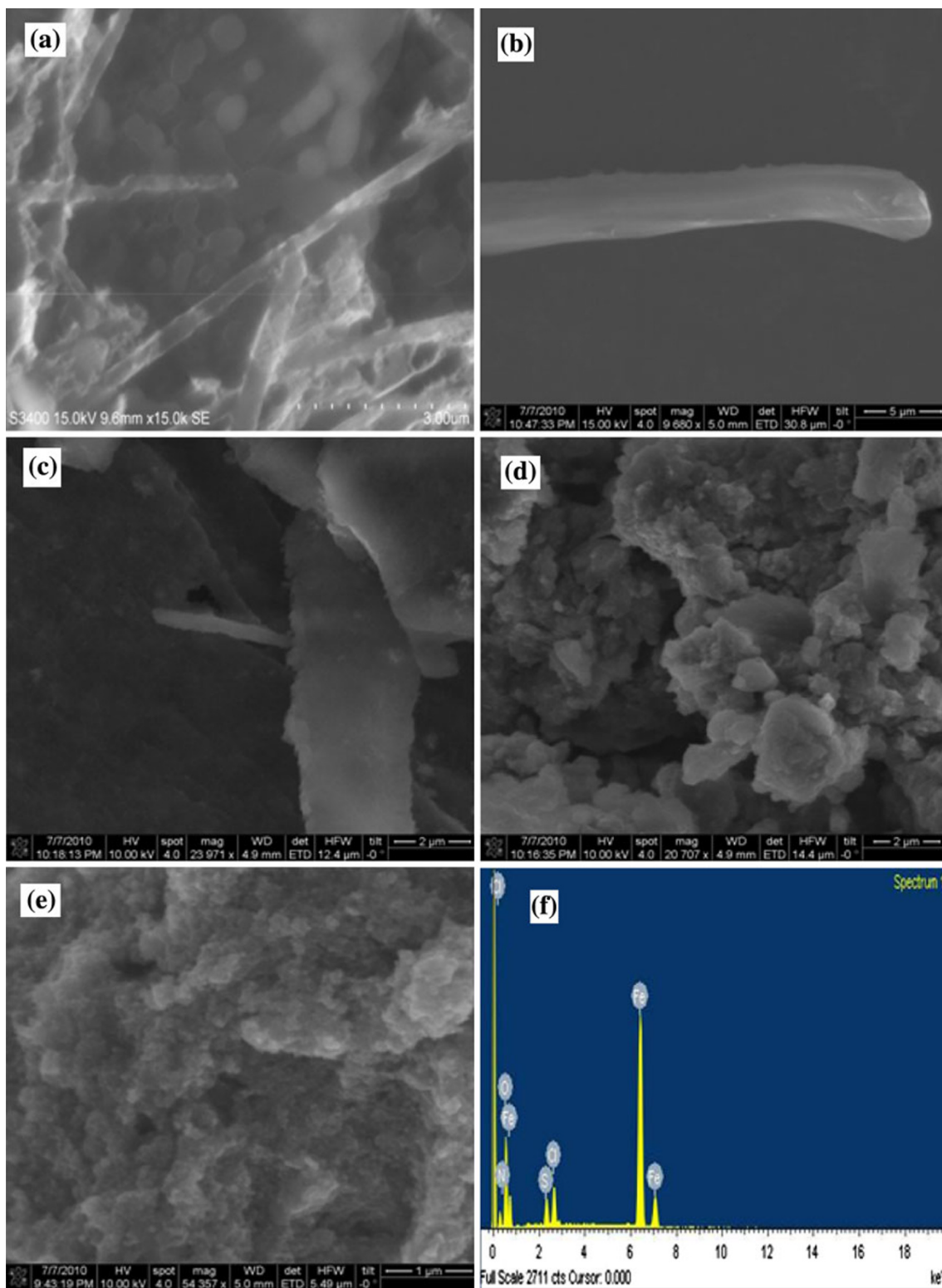


Fig. 2 SEM images of PANI/Fe₃O₄ nanocomposites prepared with **a–b** 1:5, **c** 1:4, **d** 1:3, and **e** 1:1 molar ratios of DBSA to aniline. **f** EDX of PANI/Fe₃O₄ nanocomposite

Fig. 2c–e, did not show formation of rod like structure. Concentration of DBSA to aniline apparently seems to have an influence on the morphology of nanocomposites.

Molecular structure of nanocomposite was studied by XRD, UV–Visible and FTIR spectroscopy. XRD patterns of PANI/Fe₃O₄ composites presented in Fig. 3, consists of

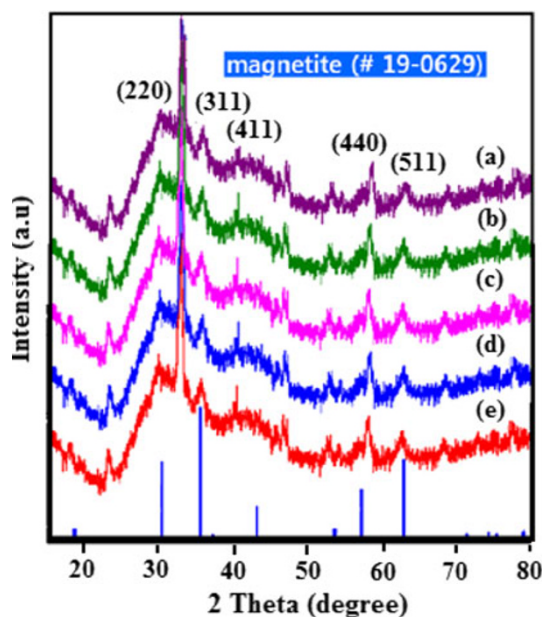


Fig. 3 XRD patterns of PANI/Fe₃O₄ nanocomposites obtained with *a* 1:1, *b* 1:2, *c* 1:3, *d* 1:4 and *e* 1:5 molar ratios of DBSA to aniline

two broad peaks at $2\theta = 21^\circ$ and 25° that can be ascribed to the periodicity parallel and perpendicular to the polymer chain of PANI (Zang et al. 2006). The diffraction patterns centered at $2\theta = 30.47^\circ$, 35.63° , 43.35° , 57.22° , 63.06° , could be indexed as (220), (311), (400), (511), and (440) planes of magnetite (JCPD file No. 19-0629).

Figure 4 shows UV–Vis spectra of PANI/Fe₃O₄ samples for different molar ratios of DBSA to aniline. It can be seen from the Fig. 4 that there are two characteristic peaks are one at 310 and other at 610 nm. The former arises due to $\pi \rightarrow \pi^*$ transitions, while the latter is due to transition of inter chain charge transfer from two adjacent benzenoid rings to the quinoid ring of PANI chain. Blue shift of both absorption bands as compared to those of pure PANI indicates some type of interaction between Ferric ions with nitrogen atom of PANI. Besides these two peaks, there is a small shoulder peak at 270 nm due to the $\pi \rightarrow \pi^*$ transition in the benzenoid rings of DBSA, confirming the presence of DBSA in the nanocomposites.

FTIR spectra of the PANI/Fe₃O₄ nanocomposites shown in Fig. 5 are in good agreement with earlier reports (Hasik et al. 2006). The characteristic peaks at $3,450$ and $3,150\text{ cm}^{-1}$ are assigned to N–H stretching vibrations of amino groups, which are indicative of $-\text{NH}_2$ groups in the structural units of the PANI rods. The strong bands at about $1,589$ and $1,496\text{ cm}^{-1}$ arise because of quinoid rings and benzenoid ring units. The presence of these bands clearly indicates that the PANI is composed of both amine and the imine units. The observed band at $1,408$ is ascribed to stretching frequency of B–N = Q moiety (where B refers to benzenoid phenyl rings and Q refers to quinoid phenyl ring) and confirms the presence of

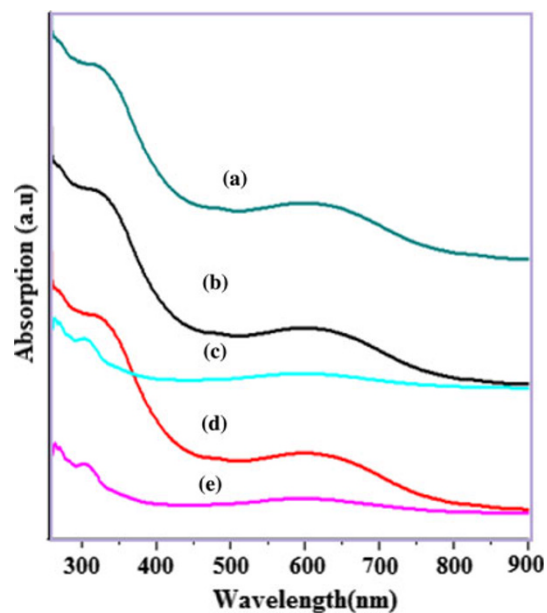


Fig. 4 UV-visible spectra of PANI/Fe₃O₄ nanocomposites prepared with *a* 1:1, *b* 1:2, *c* 1:3, *d* 1:4 and *e* 1:5 molar ratios of DBSA to aniline

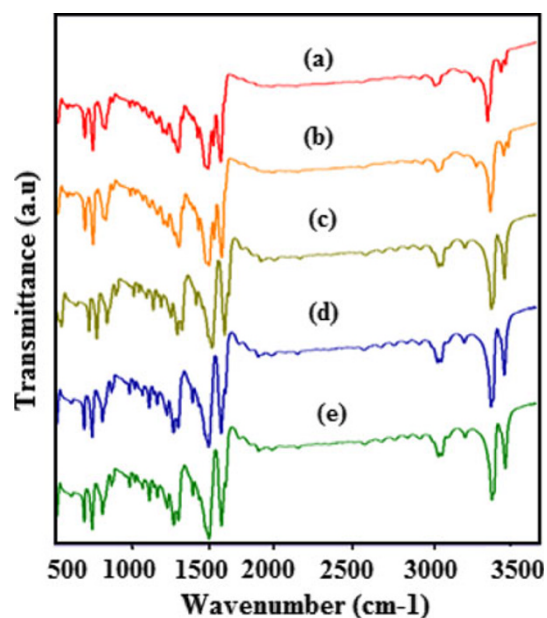


Fig. 5 FTIR spectra of PANI/Fe₃O₄ nanocomposites prepared with *a* 1:1, *b* 1:2, *c* 1:3, *d* 1:4 and *e* 1:5 molar ratios of DBSA to aniline

phenazine units. These phenazine units act as initiation centres for growth of PANI nanostructures (Kim et al. 2000). The band at $1,307\text{ cm}^{-1}$ corresponds to C–N stretching vibration mode of the 1, 4-disubstituted benzene ring of PANI. The peaks at $1,176$ and $1,132\text{ cm}^{-1}$ can be attributed to N=Q=N modes of PANI and DBSA respectively. The bands at $1,035$, 617 , and $1,008\text{ cm}^{-1}$ are due to symmetric and asymmetrical vibrations of O=S=O, S–O and C–H of DBSA which confirms

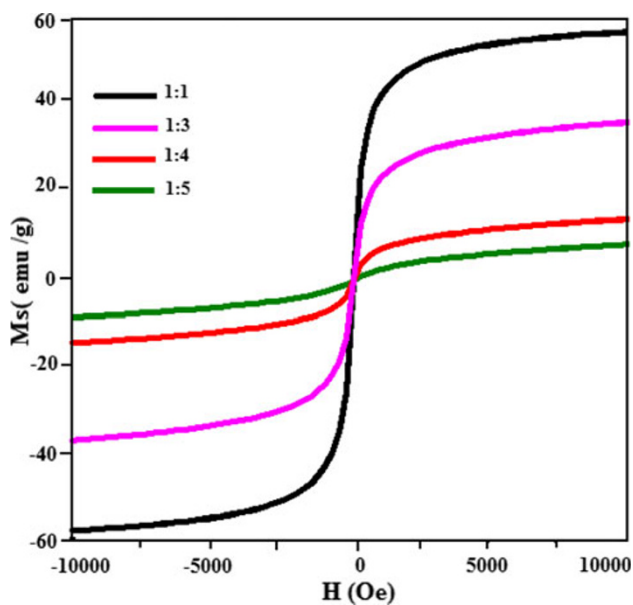


Fig. 6 Plot of magnetization as a function of field for PANI/Fe₃O₄ nanocomposites prepared with different molar ratios of DBSA to aniline

the doping of DBSA in PANI nanocomposites. The band at 831 cm⁻¹ can be attributed to the characteristic C–H out of plane bending of 1, 4-disubstituted benzene rings of PANI. Since Fe₃O₄ belongs to inverse spinel structure, Fe³⁺ ions are situated in two different lattice sites. The bands at 565 and 426 cm⁻¹ could therefore be attributed to the intrinsic Fe–O vibrations of tetrahedral and octahedral Fe³⁺, respectively. The above spectroscopic data clearly confirms that ferric ion is coordinated with the nitrogen atom of quinone rings of PANI (Waldron 1955; Wan 1989).

Figure 6 shows variation of magnetization as a function of field for PANI/Fe₃O₄ nanocomposites at room temperature. The magnetization curves are indicative of superparamagnetism as there are no hysteresis loops with remanence and coercivity. Saturation magnetization (Ms) values equal to 57, 36, 13 and 7 emu/g were obtained for the samples with 1:1, 1:3, 1:4, and 1:5 molar ratios of DBSA to aniline. These Ms values obtained were much lower than that of bulk Fe₃O₄ (Ms = 92 emu/g) (Gee et al. 2003). In general, the decrease in Ms is thought arise from the finite size effect and surface effect. But in the present case, the decrease in Ms may be attributed to substantial increase in the volume fraction of non-magnetic DBSA concentration (1:1 to 1:5).

Figure 7 depicts the thermogravimetric curves for pure PANI and PANI/Fe₃O₄ nanocomposites under nitrogen atmosphere studied at a heating rate 20 °C/min in the temperature range of 40–840 °C. Three weight loss regions were observed for pure PANI and PANI/Fe₃O₄ nanocomposite samples. The initial weight loss up to 150 °C is due to the removal of water, excess of unbound DBSA and other

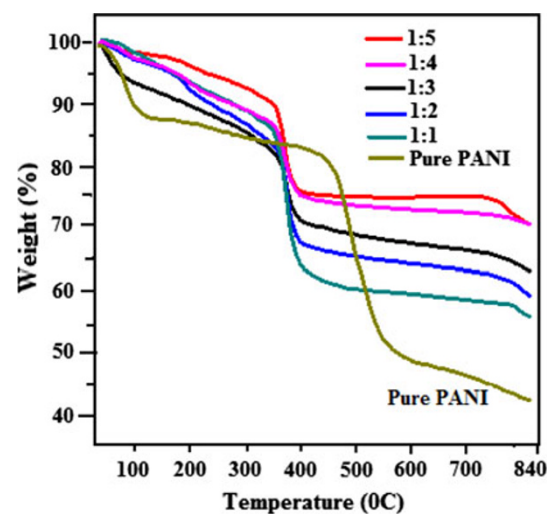


Fig. 7 Thermogram of PANI/Fe₃O₄ nanocomposites prepared with different molar ratios of DBSA to aniline

volatiles in composites. The second weight loss between 150 and 350 °C is ascribed to degradation of the bound DBSA. The third weight loss between 500 and 840 °C corresponds to degradation of PANI. The enhanced thermal stability of composites as compared to pure PANI may be due to the interaction between PANI and Fe₃O₄ NPs, which restricts the thermal motion of PANI chain in the composite.

Conclusions

We have demonstrated a simple and reproducible one-pot synthesis of PANI nanorods containing Fe₃O₄ NPs using APS as an oxidant in presence of DBSA as surfactant via in situ self-assembly method. DBSA was found to modify PANI. SEM and TEM techniques indicated that Fe₃O₄ NPs are coated on surfaces of PANI nanorods. Morphology and magnetic properties of nanocomposites were found to be critically dependent on the molar ratios of DBSA to aniline. Magnetic measurements indicated the formation of single domain particles that exhibited superparamagnetism. Thermo-gravimetric data indicated that the thermal stability of nanocomposite is higher as compared to pure PANI.

Acknowledgments K.B. thanks the University Grant Commission, India (UGC, India), and also DST-PURSE programme, Andhra University for the financial support. Y.P.K. thanks UGC, India for the award of research fellowship. The authors are grateful to Prof. T. P. Radhakrishnan and Muvva D. Prasad, Centre for nanotechnology, University of Hyderabad for providing TEM facility.

Open Access This article is distributed under the terms of the Creative Commons Attribution License which permits any use, distribution, and reproduction in any medium, provided the original author(s) and the source are credited.

References

- Bai H, Shi GQ (2007) Gas sensors based on conducting polymers. *Sensors* 7:267–307
- Bao L, Jiang JS (2005) Evolution of microstructure and phase of Fe_3O_4 in system of Fe_3O_4 -polyaniline during high-energy ball milling. *Phys B Condens Matter* 367(1–4):182–187
- Battle X, Labarta A (2002) Finite-size effects in fine particles: magnetic and transport properties. *J Phys D* 35:R15–R42
- Bhatnagar SP, Rosensweig RE (1995) Introduction to the magnetic fluids bibliography. *J Magn Magn Mater* 149:198
- Deng J, Ding X, Zhang W, Peng Y, Wang J, Long X, Li P, Chan ASC (2002) Magnetic and conducting Fe_3O_4 -cross-linked polyaniline nanoparticles with core-shell structure. *Polymer* 43:2179–2184
- Gee SH, Hong YK, Erickson DW, Park MH (2003) Synthesis and aging effect of spherical magnetite (Fe_3O_4) nanoparticles for biosensor applications. *J Appl Phys* 93:7560
- Gupta AK, Gupta M (2005) Synthesis and surface engineering of iron oxide nanoparticles for applications. *Biomaterials* 26:3995–4021
- Hasik M, Kurkowska I, Bernasik A (2006) Polyaniline incorporating cobalt ions from CoCl_2 Solutions. *React Funct Polym* 66:1703–1710
- Hatchett DW, Josowicz M (2008) Composites of intrinsically conducting polymers as sensing nanomaterials. *Chem Rev* 108:746–769
- Jeong U, Teng XW, Wang Y, Yang H, Xia YN (2007) Superparamagnetic colloids: controlled synthesis and niche applications. *Adv Mater* 19:33–60
- Kim BJ, Oh SG, Han MG, Im SS (2000) Preparation of polyaniline nanoparticles in micellar solutions as polymerization medium. *Langmuir* 16:5841–5845
- Li D, Huang J, Kaner RB (2009) Polyaniline nanofibers: a unique polymer nanostructure for versatile applications. *Acc Chem Res* 42:135–145
- Mallikarjuna NN, Manohar SK, Kulkarni PV, Venkataraman A, Aminabhavi TM (2005) Novel high dielectric constant nanocomposites of polyaniline dispersed with $\gamma\text{-Fe}_2\text{O}_3$ Nanoparticles. *J Appl Polym Sci* 97(5):1868–1974
- Marchessault RH, Richard S, Rioux P (1992) In situ synthesis of ferrites in Ignocellulosics. *Carbohydrate Res* 224:133–139
- McMichael RD, Shull RD, Swartzendruber LJ, Bennett LH, Watson RE (1992) Magnetocaloric effect in superparamagnets. *J Magn Magn Mater* 111:29–33
- Raj K, Moskowitz B, Casciari R (1995) Advances in ferrofluid technology. *J Magn Magn Mater* 149:174–180
- Raksha S, Subhalakshmi L, Annapoorni S, Parmanand S, Akihisa I (2005) Composition dependent magnetic properties of iron oxide polyaniline nanoclusters. *J Appl Phys* 97(1):014311–014316
- Reddy KR, Lee KP, Gopalan AI (2007) Novel electrically conductive and ferromagnetic composites of poly (aniline-co-aminonaphthalenesulfonic acid) with iron oxide nanoparticles: synthesis and characterization. *J Appl Polym Sci* 106:1181–1191
- Tang BZ, Geng YH, Sun QH, Zhang XX, Jing X (2000) Processible nanomaterials with high conductivity and magnetizability preparation and properties of maghemite/polyaniline nanocomposite films. *Pure Appl Chem* 72(1–2):157–162
- Ugelstad J, Berge A, Ellingsen T, Schmid R, Nilsen TN, Mork Sienstad PPC, Hornes E, Olsvik O (1992) Preparation and application of new monosized polymer particles. *Progress Polym Sci* 17:87–161
- Waldron RD (1955) Infrared spectra of ferrites. *Phys Rev* 99:1727–1735
- Wan MX (1989) The influence of polymerization method and temperature on the absorption spectra and morphology of polyaniline. *Synth Met* 31:51–59
- Wan MX, Li WC (1997) A composite of polyaniline with both conducting and ferromagnetic functions. *J Polym Sci Part A Polym Chem* 35:2129–2136
- Wang CW, Wang Z, Li MK, Li HL (2001) Well-aligned polyaniline nano-fibril array Membrane and its field emission property. *Chem Phys Lett* 341:431
- Wilson JL, Poddar P, Frey NA, Srikanth H, Mohamed K, Harmon JP (2004) Synthesis and magnetic properties of polymer nanocomposites with embedded iron nanoparticles. *J Appl Phys* 95:1439–1443
- Wu CG, Bein T (1994) Conducting polyaniline filaments in a mesoporous channel host. *Science* 264:1757–1759
- Yang QL, Zhai J, Feng L, Song YL, Wan MX, Jiang L, Xu WG, Li QS (2003) Synthesis and characterization of conducting polyaniline/ $\gamma\text{-Fe}_2\text{O}_3$ magnetic nanocomposite. *Synth Met* 135–136: 819–820
- Zang L, Wan M, Wei Y (2006) Nanoscaled polyaniline fibers prepared by ferric chloride as an oxidant. *Macromol Rapid Commun* 27:366–371
- Zhang Z, Wan M (2003) Nanostructures of polyaniline composites containing nano-magnet. *Synth Met* 132:205–212
- Zhang X, Goux WJ, Manohar SK (2004) Synthesis of polyaniline nanofibers by “Nanofiber Seeding”. *J Am Chem Soc* 126: 4502–4503